

Slotted ALOHA and CSMA Protocols for FMCW Radar Networks

Haritha K*, Vineeth Bala Sukumaran[†], Chandramani Singh*

* Indian Institute of Science, Bangalore, India

{haritha, chandra}@iisc.ac.in [†] Indian Institute of Space Science and Technology, Trivandrum, India
{vineethbs}@iist.ac.in



Abstract—We study medium access in FMCW radar networks. We assume that all the radars use the same parameters, e.g., chirp duration, chirp slope, cutoff frequency, number of chirps per packet, etc. and propose and analyze slotted ALOHA and CSMA protocols to mitigate narrowband interference. We define a notion of throughput to quantify the performance of the proposed protocols. In the case of ALOHA, we analyze interference probability and throughput as functions of the system parameters. We observe that interference probability and throughput may behave differently than in wireless communication networks. For instance, if the number of chirps per packet is larger than one, the interference probabilities may be smaller for higher transmission rates. We define a medium sensing procedure, referred to as clear channel assessment (CCA), as a part of the proposed CSMA, and also define CCA success and failure events. In CSMA, the radars transmit only after a successful CCA. We study, CCA success probability, interference probability, and throughput as functions of the system parameters. We observe that, unlike wireless communication networks, using the highest possible attempt rates may maximize throughput in a few network scenarios. We perform an extensive simulation to verify our analytical results and to compare slotted ALOHA and CSMA. We observe that CSMA outperforms ALOHA in all realistic scenarios.

1 INTRODUCTION

Self-driving cars, also referred to as driverless or autonomous cars are poised to become a reality in the next five to ten years. To ensure the safety and efficiency of transportation systems, self-driving cars must have a 360-degree view of their surrounding in a way that is ecologically and economically sustainable. These cars need various sensors such as optical cameras, millimeter-wave radars, and laser imaging detection and ranging to map the environment including cars, obstacles, and pedestrians surrounding them.

Millimeter-wave Frequency Modulated Continuous Wave (FMCW) radars [1] are long-range radars that can reliably detect distance, velocity, angle of other vehicles and objects in the vicinity self-driving cars. These radars operate in the 76-77 GHz band [2] with a bandwidth of 1 GHz. These can be made with compact antennas while retaining sufficiently high gain and narrow beamwidth to offer high range and angular resolution; they can offer localization sensitivity up to 3 cm. FMCW radar electronics are robust, and radar frequencies are generally immune to adverse weather conditions (snow/fog/rain or optical effects) [2].

For reliable operation of FMCW radars, it is imperative that received radar signals be interference-free. Interference in 76-77 GHz band will be a crucial challenge in near future in view of the likely increase in: (a) the number of self-driving cars from multiple manufacturers, (b) the number of radars per car, and (c) the operating duty cycle per radar. There are two kinds of inter-radar interference [3], [4]. (1) Wideband interference: This is applicable to heterogeneous radar networks in which different radars use different chirp slopes. This manifests itself as an increase in noise floor, leading to *signal-to-noise-ratio* (SNR) degradation, and therefore misdetection of targets. (2) Narrowband interference: this happens if a radar has another (interfering) radar using the same chirp slope in its vicinity and the beat signal frequency due to interfering radar is less than the cut-off frequency of the Low Pass Filter (LPF). This causes ghost detections (or, false alarms) [1]. Both types of interference deteriorate radar performance, but mitigation of narrowband interference requires signal processing as well as medium access techniques [5]. In this work, we focus on the mitigation of narrowband interference using medium access techniques. In this work, we focus on the mitigation of narrowband interference.

Medium access techniques have been widely studied in the context of wired and wireless communication networks. In communication networks, if a node receives signals from two simultaneously transmitting nodes, it cannot decode any of the signals; this phenomenon is termed as collision. A number of centralized (e.g., TDMA) and distributed (e.g., ALOHA, CSMA, CSMA-CA) multiple access protocols have been proposed to minimize interference in communication networks. In the context of FMCW radars, medium access control can reduce false alarms but may also lead to missed targets. Design and analysis of medium access control protocols is pivotal for large scale deployment of radar networks.

1.1 Related work

Jin et al. [6] considered a network of FMCW radars with identical chirp parameters and obtained statistical characterizations of interference signal properties under an asynchronous pure random access scheme. A received chirp is classified as a false alarm or a real target based on its

received power. Further, they considered continuous time setup and the radars chose transmission start time randomly and after that, they transmit chirps continuously. In our work, we consider slotted time structure and there is a random time duration between the successive packets.

In [7] and [8] the authors use carrier sensing to mitigate the interference. Ishikawa et al. [7] considered collocated radars with identical parameters. The authors proposed a carrier sense multiple access (CSMA) algorithm to avoid the interference of FMCW radar signals by shifting the transmission timing after sensing the medium. But, they do not analyze the performance of the algorithm when the radars are non-collocated. We propose a variant of CSMA and discuss its performance in both collocated and non-collocated radar networks.

Ammen et al. [8] propose a technique that generates an interference replica of the ghost signal during carrier sensing. This is subtracted from the received signal in the frequency spectrum to mitigate narrowband interference.

To mitigate narrowband interference different techniques, e.g., TDM, FDM, phase coding, frequency hopping, and chirp sequence are used to orthogonalize the chirp transmissions in [9], [10], [11], [4], [12], [13], and [14].

Centralized medium access mechanisms for radars were proposed in [12] and [13]. In [12], a control center was setup to receive speed and location information from all the nearby radars. Using these the controller computes the waveform parameters that provide orthogonal access to the medium and dispatches them to each one to avoid interference. In [13], the authors proposed a resource allocation strategy that relies on the existing communication infrastructure to jointly assign slope directions and carrier frequency offset to all the radar units operating in its vicinity.

Aydogdu et al. [9] proposed a medium access control protocol RadChat. It is a coordinated framework among the nearby vehicles and uses time division and frequency division techniques to mitigate interference caused by neighboring radars. The schemes discussed in [9] and [12] use time synchronous orthogonal techniques to avoid interference. The challenge in these time synchronous schemes is propagation delay ($\approx \mu\text{s}$) can deteriorate the efficacy of orthogonality.

Son et al. [14] proposed an algorithm where they assign a chirp sequence for FMCW radar. They design a chirp sequence set such that the slope of each vehicle's chirp sequence will not overlap within the set. By assigning one of the chirp sequences to each vehicle, interference can be mitigated.

Jin et al. [10] proposed asynchronous non-cooperative protocols to mitigate interference in radars. They quantify the network performance using cross layer performance metrics such as multiple access capacity and target mis-detection probability. They explore different combination of frequency hopping, phase coding, and random frequency division multiple access techniques to avoid interference.

Luo et al. [11] proposed a frequency-hopping random chirp technique that reconfigures the chirp sweep frequency and time in every cycle. This results in a noise-like frequency response after the received signal is demodulated at the receiver. Rao et al. [4] used clock drift that changes the slope

of interfering radar with respect to the tagged radar. Further, they employ binary phase encoding to mitigate interference.

Al-Hourani et al. [15] considered a Poisson point process and a Bernoulli lattice process as models for the spatial distribution of radars. Using stochastic geometry they compute interference statistics and obtain analytical expressions for the probability of successful range estimation.

1.2 Our Contribution

We consider slotted ALOHA protocol, wherein the radar transmits for a fixed amount of time and enters into backoff state. We propose CSMA, in which each radar senses the medium before transmitting the packet.

- We derive the probability of interference in FMCW radar networks assuming that all the radars are synchronized and collocated in ALOHA.
- We also derive the probability of interference in the scenario where the radars are not collocated and their clocks are not synchronized, i.e., each pair of radars is associated with a non-zero propagation time in ALOHA.
- In both the cases, as expected, the interference probability increases with medium access probability if the number of chirps per packet is one. However, if packets consist of more than one chirp, the interference probability first increases and then decreases with medium access probability.
- We define a notion of throughput and derive throughput for both of the above scenarios. If each packet consists of exactly one chirp, the throughput first increases and then decreases with medium access probability. In this case, we derive the expression for the optimal medium access probability. When the packets consist of more than one chirp the throughput first increases and reaches the maximum, then decreases and increases with medium access probability.
- We propose a CSMA protocol that senses the medium before transmitting a packet. we define a medium sensing procedure called clear channel assessment (CCA) and CCA success and failure events. Further, we analyze the CSMA protocol using fixed point analysis for a restricted class of radar networks.
- We perform extensive simulation to verify our analytical results and to compare slotted ALOHA and CSMA.

Organization of the paper: We explain the operation of a FMCW radar in Section 2.1 and introduce the system model in Section 2.2. In Section 3 we analyze slotted ALOHA and derive the probability of interference and throughput. In Section 4 we propose CSMA protocol. In Sections 4.1 and 4.2 we analyze CSMA in collocated and non-collocated radar networks respectively. In Section 5 we verify our analytical results obtained and compare the performance of slotted ALOHA and CSMA protocols.

2 SYSTEM MODEL

2.1 FMCW Radars

In this section we explain the operation of a FMCW radar and narrowband interference using radar transmit/receive

block Figure 1 [6]. The FMCW radar is used to measure the range, velocity, and angle of arrival of a target in front of it. The radar generates a sinusoid signal called chirp whose frequency increases linearly with time. The chirp is characterized by following parameters, starting frequency (f_{\min}), ending frequency (f_{\max}), bandwidth (B), chirp duration (T_c), and slope ($h = \frac{B}{T_c}$) as shown in Figure 2.

To explain the operation of FMCW radar we consider a single target in front of the radar at distance d . The MAC scheduler schedules the chirps transmissions and the synthesizer generates the chirps at these scheduled times. The transmitting antenna transmits them. The reflected chirp from the target is received by receiving antenna with a delay $\tau = \frac{2d}{c}$. The reflected and transmitted chirps are given as inputs to a mixer. The mixer is a device that takes two sinusoids as inputs and generates another sinusoid whose instantaneous frequency is equal to the absolute difference of instantaneous frequencies of the input signals. Note that the reflected chirp is delayed by $h\tau$ from the transmitter chirp as shown Figure 2. The target at distance d generates an IF signal with frequency $\frac{2dh}{c}$ at the output of the mixer. This is further passed through a LPF with cut-off frequency f_H . The cut-off frequency is a function of the sampling frequency of the ADC. The IF signal is further digitized using ADC and converted into frequency domain using DFT. The detector detects a peak at frequency $\frac{2dh}{c}$. Note that the maximum frequency that can be observed is limited by the cut-off frequency of the LPF. This leads to,

$$\begin{aligned} h\tau &< f_H \\ \tau &< \frac{f_H}{h} \text{ and } d < \frac{cf_H}{2h}. \end{aligned} \quad (1)$$

Target range (d_{\max}): The maximum distance between the radar and the target such that the corresponding IF signal is passed through the LPF. This is given by $\frac{cf_H}{2h}$.

Slot (Δ): The maximum round trip delay between the radar and the target such that the corresponding IF signal is passed through LPF and is given by f_H/h .

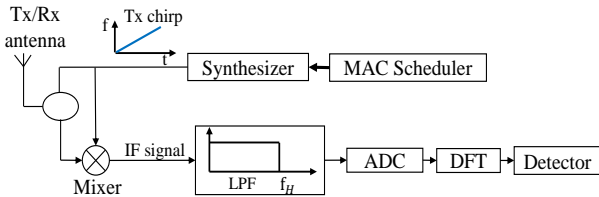


Fig. 1. TX/RX block diagram for a FMCW radar

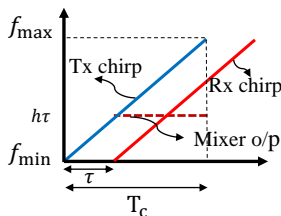


Fig. 2. Illustration of the transmitted chirp, received chirp, and the IF signal obtained by mixing

Multiple targets in front of radar: Now consider the scenario where there are two targets in front of the radar with in the target range and we want to compute their distance from the radar. Let d_1, d_2 be the distances from the radar. Ideally we should be able to observe two peaks in the frequency spectrum at $\frac{2hd_1}{c}, \frac{2hd_2}{c}$ corresponding to the targets at distance d_1, d_2 respectively. The maximum amount of time available to observe the reflected chirps is T_c (see Figure 2). This observation window T_c can distinguish frequency components that are separated by more than $\frac{1}{T_c}$ Hz [1]. So, to observe two peaks corresponding to the distances d_1 and d_2 in the frequency spectrum,

$$\begin{aligned} \frac{2hd_1}{c} - \frac{2hd_2}{c} &> \frac{1}{T_c} \\ d_1 - d_2 &> \frac{c}{2B} \end{aligned} \quad (2)$$

where B is the bandwidth of the chirp.

Range Resolution (Δd): Range resolution is the minimum distance between the two targets such that the radar can distinguish them and it is given by $\Delta d = \frac{c}{2B}$.

Remark 2.1. If the distance between two targets is less than the range resolution then we observe only a single peak in the DFT spectrum and radar detects them as a single target.

False alarm or interference: Now consider two FMCW radars with identical parameters and separated by a distance d . Let us label these as first radar and second radar respectively. Each radar receives chirps transmitted by the other radar as shown in Figure 3.

Let t_1, t_2 be the start times of chirps at the first radar and the second radar respectively. Then at time $t_3 = t_2 + \frac{d}{c}$ the first radar receives the chirp transmitted by the second radar. If $\tau = |t_1 - t_3| < \Delta$ (see Figure 3a) a signal at frequency $f_{IF} = h\tau$ is observed at the output of LPF. Note that the first radar assumes the chirp received from the second radar as reflected version of its own chirp and computes the distance. The first radar assumes that there is a target at distance $d_g = \frac{cf_{IF}}{2h}$. We call this a ghost target because there is no real target at this distance. The phenomenon of a radar detecting a ghost target is called a *false alarm*. We also call this *interference*. Note that the first radar does not observe a false alarm for every chirp received from the second radar. The following time condition has to be satisfied to observe a false alarm at the first radar.

$$t_1 - \Delta < t_2 + \frac{d}{c} < t_1 + \Delta. \quad (3)$$

We define the *Interference range* ($d_{I,\max}$) as the maximum distance between two radars such that the interference is observed. It is a function of chirp power transmitted by the second radar. Any radar outside the interference range contributes no interference.

2.2 FMCW Radar Networks

We consider a network of M radars with identical chirp parameters. The radars operate using a slotted time structure with slot size Δ . We assume that the chirp duration is an integer multiple of slot size, i.e., $T_c = K\Delta$, where K is a positive integer. Further, we define the clock offset $\delta_{k,l}$ of radar l with respect to radar k as the time duration between

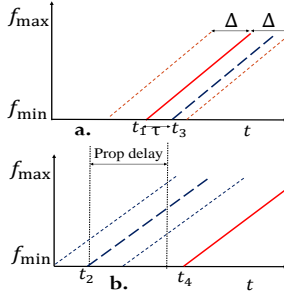


Fig. 3. Illustration of a "ghost target" being detected at radar 1. In (a) and (b) we illustrate the transmitted and received chirps of radars 1 and 2. If a radar (radar 1) receives a transmission within $(t_1 - \Delta, t_1 + \Delta)$ then we have interference and a ghost target is detected.

Symbol	Description
f_{\min}	Chirp starting frequency
f_{\max}	Chirp ending frequency
B	Chirp bandwidth
h	Chirp slope
T_c	Chirp duration in seconds
M	Number of radars
K	Chirp duration in number of slots
L	Number of chirps per packet
W	Number of backoff slots

TABLE 1
Notations and symbols used

a radar k 's clock tick and a radar l 's clock tick that comes immediately after radar k 's clock. Note that $\delta_{k,l} \in [0, \Delta)$. We call a network *synchronous* if $\delta_{k,l} = 0, \forall k, l \in \{1, 2, \dots, M\}$ else we call it *asynchronous*. As described in Section 2.1, radars' transmissions interfere with each other. The radars employ a MAC protocol to schedule their transmissions for the possible reduction of interference. In general, in a MAC protocol, each radar interleaves transmissions with silence periods, termed as backoffs. The backoff durations are random whereas a fixed number of, say L , chirps are contiguously transmitted before going for the next backoff. We refer to the contiguous sequence of L chirps as a packet.

We introduce two MAC protocols, namely slotted ALOHA and CSMA, in Sections 3 and 4, respectively. Here, we define a metric, called throughput, to quantify the performance of a MAC protocol. It is the fraction of time slots spent by all the radars in transmitting packets successfully without interference.

Throughput (Θ): Let $S(T)$ be the total number of packets transmitted successfully by all the radars in a network in T slots. Then the throughput of the network is given by,

$$\Theta = \lim_{T \rightarrow \infty} \frac{KL S(T)}{T}, \quad (4)$$

where K is the chirp length in slots and L is the number of chirps per packet.

Effect of backoff on target detection: Let us define a backoff and the subsequent packet transmission as a transmission cycle (see Figure 4). The length of a transmission cycle is typically much shorter than d_{\max}/v_{\max}

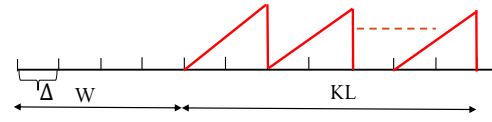


Fig. 4. Transmission cycle

where v_{\max} is the maximum relative speed of the target; it is the time derivative of the distance between the radar and the target. For instance, consider the following example with typical radar parameters and vehicle speeds [7]. The slot $\Delta = \frac{4}{3} \times 10^{-6}$ s and $d_{\max} = 200$ m. Let W be the number of backoff slots. The change in distance between target and radar in this duration is $\Delta W v_{\max}$ meters. We consider typical values, $v_{\max} = 50$ m/s (180kmph), $W = 100$. The distance traveled by the target in W slots is 0.67cm. We have used typical values for radar parameters and vehicle speeds in this calculation, the actual values may differ but would be of the same order. Consider a target just entered into the radar range when the radar is in backoff state. Let d be the distance between them. The change in d before and after backoff is at most in the order of centimeters and very small compared to $d_{\max} \approx 200$ m. So, it takes several transmission cycles for a target to come alarmingly close to the radar after it enters the transmission range of the radar. Therefore, the radars are unlikely to miss the targets because of backoffs.

We tabulate the symbols and notations used in TABLE 1. Further, we use $\mathbb{E}[\cdot]$ for expectation and Geo(p) for geometric distribution with parameter p .

3 SLOTTED ALOHA

Slotted ALOHA: We consider a slotted ALOHA protocol wherein each radar transmits L chirps contiguously and enters into backoff for W slots (see Figure 4) and repeats the same. Successive backoffs constitute a sequence of independent and identically distributed (i.i.d) random variables, each having cumulative distribution function F . Let W denote a generic random variable with distribution F . We assume that $\mathbb{E}[W]$ is finite. In ALOHA each radar transmits packets irrespective of the other radars' transmissions in the network. So, each radar's packets can be interfered by other radars' packets.

In this section, we analytically characterize the throughput of slotted ALOHA using the probability of interference. We assume all radars in the network have identical chirp parameters. Further, the clock offset of radar l with respect to radar k is given by $\delta_{k,l}$ and the distance between them is given by $d_{k,l}$. We compute the probability of interference in the following network scenarios.

- 1) We assume that all the M radars are collocated, i.e., we ignore the propagation delays and that their clocks are synchronized i.e., $\delta_{k,l} = 0$, for all k, l . We use the insights from this scenario to analyze the second scenario, described below.
- 2) We assume that all the M radars are non-collocated and each radar $k, k \in \{1, \dots, M\}$ can potentially interfere with all the other radars $l, l \in \{1, \dots, M\} \setminus k$ in the network. Further, we assume clocks are not synchronized.

In order to derive the probability of interference, we define the state of a radar in a slot as follows. We say that a radar is in state 0 if it is in backoff. Further, if a radar is transmitting i -th slot in the packet then we say that it is in state i , $i \in \{1, \dots, KL\}$. Recall that in ALOHA protocol each radar transmits packets irrespective of other radars' packet transmissions. So, the state evolution of each radar is independent of other radars. Let us define $\pi = (\pi_0, \pi_1, \pi_2, \dots, \pi_{KL})$ where $\pi_i, i \in \{0, 1, \dots, KL\}$ is long term fraction of slots the radar spends in state i . We evaluate π in the following and use it in the Propositions 1, 2 and 3 to compute the probability of interference and throughput.

The radar's state evolves according to a renewal process with the slots in which the radar state is 1 being the renewal epochs. The duration of a transmission cycle $C_i, i \in \{1, 2, \dots\}$ is random and independent across i . Further, $\mathbb{E}[C_i] = KL + \mathbb{E}[W]$. With this we define renewal epochs at a radar

$$Z_j = \sum_{i=1}^j C_i, \text{ and } Z_0 = 0$$

and renewal process

$$\phi(T) = \sup\{j \geq 0 : Z_j \leq T\},$$

where $\phi(T)$ denotes the number of radar transmission cycles occurred until time slot T . Let R_i be the reward associated with i -th transmission cycle. The total reward earned in $\phi(T)$ cycles is given by

$$R(T) = \sum_{i=1}^{\phi(T)} R_i(T).$$

We define this reward as the amount of time the radar has spent in transmitting chirps i.e., $R_i = KL, i \in \{1, 2, \dots, \phi(T)\}$. From the Elementary Renewal theorem and Renewal Reward theorem [16]

$$\begin{aligned} \lim_{T \rightarrow \infty} \frac{\phi(T)}{T} &= \frac{1}{KL + \mathbb{E}[W]} \text{ almost surely,} \\ \lim_{T \rightarrow \infty} \frac{R(T)}{T} &= \frac{KL}{KL + \mathbb{E}[W]} \text{ almost surely.} \end{aligned} \quad (5)$$

We defined

$$\pi_i = \lim_{T \rightarrow \infty} \frac{\text{The amount time spent in state } i \text{ until slot } T}{T},$$

using (5) in above we write,

$$\begin{aligned} \pi_0 &= \frac{\mathbb{E}[W]}{KL + \mathbb{E}[W]}, \\ \pi_1 &= \pi_2 = \dots = \pi_{KL} = \frac{1}{KL + \mathbb{E}[W]}. \end{aligned} \quad (6)$$

Now we consider the scenarios described at the beginning of this section to compute interference probability. First, we compute the probability of interference in two radar network and using this result we compute in M radar network. In two radar network we label the radar at which we are observing as tagged radar and the other one as interfering radar. Let d and δ be the distance between the two radars and clock offset of interfering radar with respect to the tagged radar respectively. We first consider synchronous and collocated radar network. We consider asynchronous and non-collocated radar network subsequently.

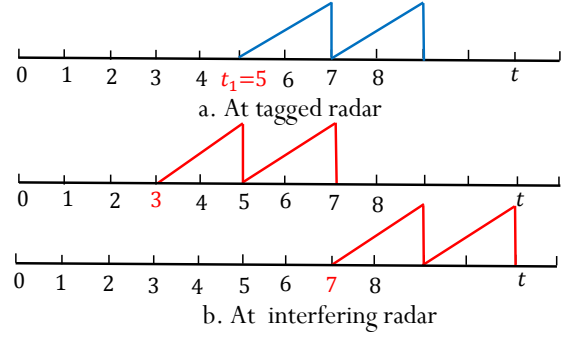


Fig. 5. Illustrating the interference events E_{-1}, E_1 for $K = 2, L = 2$. a. The tagged radar transmitting a packet, b. Interfering events at the interfering radar

3.1 The case $\delta = 0, d = 0$

In this case the time condition (3) for interference at the tagged radar in the slotted system reduces to

$$t_1 - 1 < t_2 < t_1 + 1,$$

where t_1, t_2 indicate chirp start time slot indices at the tagged and interfering radars respectively. As t_1, t_2 are integers the above condition gives $t_1 = t_2$, i.e., if two chirps at the tagged and interfering radars start at the same slot then tagged radar suffers interference. Recall that (see Figure 4) each radar transmits L -chirps contiguously in one transmission cycle. So, the interference can be caused by any one of the L -chirps from interfering radar to any one of the L -chirps at the tagged radar as shown in Figure 5. Further, we say that a packet is successfully transmitted if none of its chirps are interfered by the packets from other radars.

Without loss of generality let us assume a packet transmission started at the tagged radar at slot t_1 . Let us define following events at the interfering radar $\{E_{-(L-1)}, \dots, E_0, E_1, \dots, E_{L-1}\}$ where event $E_i, i \in \{-(L-1), \dots, L-1\}$ is starting packet transmission at slot $t_1 + iL$. Further, observe that these are the only events that can cause interference at the tagged radar.

This is explained for the case $L = 2$ in Figure 5. The interfering events possible in are $\{E_{-1}, E_0, E_1\}$. We have shown events E_{-1}, E_1 starting packet transmission at slots $t_1 - 2, t_1 + 2$ respectively. In the case of E_{-1} first and second chirps from the tagged and interfering radars started at the same slot. Similarly, in E_1 , second and first chirps from tagged and interfering radars started at the same slot.

Given the tagged radar started transmission cycle at slot t_1 the only events that can cause interference are $\{E_{-(L-1)}, \dots, E_0, E_1, \dots, E_{L-1}\}$. From (6) we have the probability of starting packet transmission in any slot is $\mathbb{P}(E_i) = \frac{1}{KL + \mathbb{E}[W]}, i \in \{-(L-1), \dots, L-1\}$. Using this we define the probability of interference at the tagged radar as

$$p_{I2} = \mathbb{P}\left(\bigcup_{i=-(L-1)}^{L-1} E_i\right).$$

In Proposition 1, we derive the probability of interference at the tagged radar in two radar network and extend that to the case of a M -radar network.

Proposition 1. 1) The interference probability at the tagged radar in two radar network is given by, □

$$p_{I2} = \frac{2L-1}{KL + \mathbb{E}[W]} - \frac{1}{KL + \mathbb{E}[W]} \sum_{i=1}^{L-1} (L-i) \mathbb{P}(W = (i-1)K).$$

2) The interference probability at the tagged radar in M radar network is given by,

$$p_I = 1 - (1 - p_{I2})^{M-1}.$$

Proof: We observe that $\{E_{-(L-1)} \dots E_0\}$ are mutually exclusive and $\{E_0, \dots, E_{(L-1)}\}$ are mutually exclusive. Further, $E_i, i \in \{1, \dots, L-1\}$ and $E_{-(L-j)}, j \in \{1, \dots, i\}$ are not mutually exclusive. Now consider,

$$\begin{aligned} p_{I2} &= \mathbb{P}\left(\bigcup_{i=-(L-1)}^{L-1} E_i\right) \\ &= \sum_{i=-(L-1)}^{L-1} \mathbb{P}(E_i \setminus (\bigcup_{j=-(L-1)}^{i-1} E_j)) \\ &\stackrel{(a)}{=} \sum_{i=-(L-1)}^0 \mathbb{P}(E_i) + \sum_{i=1}^{L-1} \mathbb{P}(E_i \setminus (\bigcup_{j=-(L-1)}^{i-1} E_j)) \\ &= \sum_{i=-(L-1)}^{L-1} \mathbb{P}(E_i) - \mathbb{P}\left(E_i \cap (\bigcup_{j=-(L-1)}^{i-1} E_j)\right) \\ &\stackrel{(b)}{=} \sum_{i=-(L-1)}^{L-1} \mathbb{P}(E_i) - \sum_{i=1}^{L-1} \sum_{j=1}^i \mathbb{P}(E_i \cap E_{-(L-j)}). \quad (7) \end{aligned}$$

The (a) and (b) follows from mutually exclusive nature of $\{E_{-(L-1)} \dots E_0\}$ and $\{E_1, \dots, E_{(L-1)}\}$ respectively. Now consider second term from the above.

$$\begin{aligned} &\sum_{i=1}^{L-1} \sum_{j=1}^i \mathbb{P}(E_i \cap E_{-(L-j)}) \\ &= \sum_{i=1}^{L-1} \sum_{j=1}^i \mathbb{P}(E_{-(L-j)}) \mathbb{P}(E_i | E_{-(L-j)}) \\ &= \frac{1}{KL + \mathbb{E}[W]} \sum_{i=1}^{L-1} \sum_{j=1}^i \mathbb{P}(W = (i-j)K) \\ &= \frac{1}{KL + \mathbb{E}[W]} \sum_{i=1}^{L-1} (L-i) \mathbb{P}(W = (i-1)K). \end{aligned}$$

In the second equality follows from (6) and given $E_{-(L-j)}$, E_i takes place if backoff duration (W) is exactly $(i-j)K$ slots. Using above in (7) gives

$$p_{I2} = \frac{2L-1}{KL + \mathbb{E}[W]} - \frac{1}{KL + \mathbb{E}[W]} \sum_{i=1}^{L-1} (L-i) \mathbb{P}(W = (i-1)K). \quad (8)$$

The probability of tagged radar suffering no interference in two radar network is given by $1 - p_{I2}$, and in M independent radar network is given by $(1 - p_{I2})^{M-1}$. So, the probability of interference at the tagged radar in M radar network is,

$$p_I = 1 - (1 - p_{I2})^{M-1}.$$

Remark 3.1. If the distance between the tagged and interfering radars is $d = j\Delta c, j \in \{0, 1, \dots\}$, we have the same expression for p_{I2} .

3.2 The case $\delta > 0, d \geq 0$

Consider the two radar system with $\delta \in [0, \Delta], d > 0$. The time condition for interference (3) at the tagged radar in this scenario reduces to

$$(t_1 - 1)\Delta < t_2\Delta + \delta + \frac{d}{c} < (t_1 + 1)\Delta,$$

where t_1, t_2 are chirp start time slot indices of tagged and interfering radars, d is distance and δ is the clock offset at interfering radar with respect to the tagged radar. Now consider above time condition, and let $\delta_1 = \delta + \frac{d}{c}$.

$$\begin{aligned} (t_1 - 1)\Delta &< t_2\Delta + \delta_1 < (t_1 + 1)\Delta \\ (t_1 - 1) - \frac{\delta_1}{\Delta} &< t_2 < (t_1 + 1) - \frac{\delta_1}{\Delta}. \end{aligned}$$

As t_1, t_2 are integers,

$$t_2 = t_1 - 1 - \left\lfloor \frac{\delta_1}{\Delta} \right\rfloor \text{ or } t_1 + 1 - \left\lceil \frac{\delta_1}{\Delta} \right\rceil. \quad (9)$$

Observe that irrespective of the exact values of d, δ chirp start slot index t_2 can take two successive integers values. If the chirp at the interfering radar starts at any of these two slot indices then tagged radar suffers interference. Note that in the first scenario $d = 0, \delta = 0$ (Section 3.1) the number of possible slot indices that can cause interference was only one.

Now we define events similar to the one defined in Section 3.1 that can cause interference at the tagged radar. Without loss of generality let us assume a packet transmission started at the tagged radar at time slot t_1 . Let us define events $\{E_{-(L-1)}, \dots, E_{L-1}\}$ at the interfering radar, where event $E_i, i \in \{-(L-1) \dots L-1\}$ is starting packet transmission at slot

$$t_1 + iK - 1 - \left\lfloor \frac{\delta_1}{\Delta} \right\rfloor \text{ or } t_1 + iK + 1 - \left\lceil \frac{\delta_1}{\Delta} \right\rceil.$$

These are the only events that can cause interference at the tagged radar.

For example consider $L = 2, K = 2, \delta = 0.5\Delta, d = 0.2c\Delta$, so $\delta_1 = 0.7\Delta$. Consider E_0 , transmission cycle at interfering starts at slot $t_2 = t_1 - 1$ or $t_2 = t_1$. Similarly for E_1 , the transmission cycle starts at $t_2 = t_1 + 1$ or $t_1 + 2$ as explained in Figure 6. We compute the probability of these events in Lemma 3.1.

Lemma 3.1. The probability of event $E_i, i \in \{-(L-1) \dots L-1\}$ is given by

$$\mathbb{P}(E_i) = \begin{cases} \frac{2}{KL + \mathbb{E}[W]} & \text{for } KL > 1 \\ \frac{1}{1 + \mathbb{E}[W]} + \frac{1 - \mathbb{P}(W=0)}{L + \mathbb{E}[W]} & \text{for } KL = 1. \end{cases} \quad (10)$$

Proof: First we consider the case $KL = 1$. In this case we have only one chirp of length one slot in each transmission cycle. Let t_1 be the start of packet transmission at the tagged radar. From (9) we have two successive slots in which if the packet transmission starts at the interfering radar the tagged radar suffers interference. Let us call these

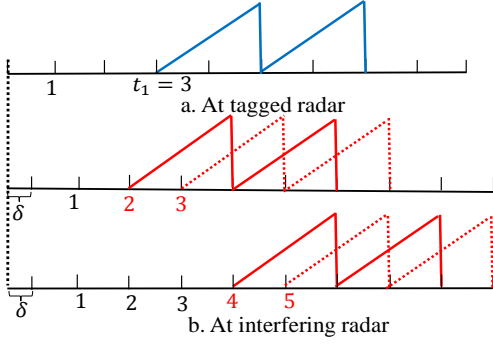


Fig. 6. Illustrating the interference events E_0, E_1 for $K = 2, L = 2$, a. The tagged radar transmitting a packet, b. Interfering events at the interfering radar

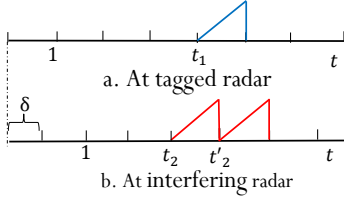


Fig. 7. Illustrating the interference event E_0 for $KL = 1$, a. The tagged radar transmitting a packet, b. Interfering events at the interfering radar

t_2, t'_2 . Observe that when $KL = 1$, two consecutive packets can start in t_2, t'_2 if the backoff duration is zero between them as shown in Figure 7b. Note that if $KL > 1$ two consecutive packets can not start in any two successive slots. The event E_i is defined as the packet starting in any one of these slots.

In order to compute $\mathbb{P}(E_i)$ let us define the state of a radar in a slot as follows. We say that the radar is in state 0 if it is transmitting. Further, we say that it is in state j if it is in j -th consecutive backoff slot. Note that the latter case arises only if the radar is in the middle of a backoff of length greater than or equal to j . Also, notice that these definitions of states are different from those in Section 3. Let us define α_j to be the long term fraction of slots the radar spends in state j . The radar's state evolves according to a renewal process with the slot in which the radar is in state 0 being the renewal epochs. We can therefore derive α_j , for $j \geq 1$ as follows.

$$\begin{aligned} \alpha_j &= \lim_{T \rightarrow \infty} \frac{\text{No. of transmission cycles until slot } T}{T} \mathbb{P}(W \geq j) \\ &= \frac{\mathbb{P}(W \geq j)}{1 + \mathbb{E}[W]}, \end{aligned}$$

the last equality follows from Elementary Renewal theorem [16].

Now consider the event E_i at interfering radar i.e., starting the chirp at slot t_2 or radar is in the last time slot of the backoff at slot t_2 , (this automatically makes $t'_2 = t_2 + 1$ chirp starting slot). Probability of starting chirp in t_2 is given by $\frac{1}{1 + \mathbb{E}[W]}$. Now the probability of t_2 being the last slot of backoff is given by

$$\sum_{j \geq 1} \alpha_j \frac{\mathbb{P}(W = j)}{1 - F(j-1)}.$$

Using these two we compute $\mathbb{P}(E_i)$.

$$\begin{aligned} \mathbb{P}(E_i) &= \mathbb{P}(\text{transmission cycle starting at slot } t_2 \text{ or } t_2 + 1) \\ &= \frac{1}{1 + \mathbb{E}[W]} + \sum_{i \geq 1} \alpha_j \frac{\mathbb{P}(W = j)}{1 - F(j-1)} \\ &= \frac{1}{1 + \mathbb{E}[W]} + \frac{1 - \mathbb{P}(W = 0)}{1 + \mathbb{E}[W]} \end{aligned}$$

Now consider $KL > 1$. In this case the packet transmission starting slots at t_2 and $t_2 + 1$ are mutually exclusive events and from (6) we write $\mathbb{P}(E_i) = \frac{2}{KL + \mathbb{E}[W]}$. \square

Using the $\mathbb{P}(E_i), i \in \{-(L-1) \dots L-1\}$ derived in Lemma 3.1 we derive the probability of interference at the tagged radar in two radar network and M radar network in Proposition 2.

Proposition 2. 1) The probability of interference at the tagged radar in two radar network is given by,

$$\begin{aligned} p_{I2} &= (2L-1)\mathbb{P}(E_1) \\ &\quad - \frac{1}{KL + \mathbb{E}[W]} \sum_{i=0}^{L-2} (L-i-1) \left(2\mathbb{P}(W = iK) \right. \\ &\quad \left. + \mathbb{P}(W = iK+1) + \mathbb{P}(W = iK-1) \right). \end{aligned}$$

where $\mathbb{P}(E_i)$ is given by (10).

2) The probability of interference at the tagged radar in M radar system is given by,

$$p_I = 1 - (1 - p_{I2})^{M-1}.$$

Proof. Using similar arguments as in the proof of Proposition 1 we have,

$$\begin{aligned} p_{I2} &= \mathbb{P}\left(\bigcup_{i=-(L-1)}^{L-1} E_i\right) \\ &= \sum_{i=-(L-1)}^{L-1} \mathbb{P}(E_i) - \sum_{i=1}^{L-1} \sum_{j=1}^i \mathbb{P}(E_i \cap E_{-(L-j)}). \end{aligned} \quad (11)$$

Now consider the second term from above,

$$\begin{aligned} &\mathbb{P}(E_i \cap E_{-(L-j)}) \\ &= \mathbb{P}(E_{-(L-j)}) \mathbb{P}(E_i | E_{-(L-j)}) \\ &= \frac{1}{KL + \mathbb{E}[W]} \left(2\mathbb{P}(W = (i-j)K) \right. \\ &\quad \left. + \mathbb{P}(W = (i-j)K-1) + \mathbb{P}(W = (i-j)K+1) \right) \end{aligned}$$

Using above in (11), we get p_{I2} .

Using the similar arguments as in the proof of Proposition 1 we have,

$$p_I = 1 - (1 - p_{I2})^{M-1}. \quad \blacksquare$$

3.3 Throughput

We compute the throughput we defined in Section 2.2 in the following Proposition 3.

Proposition 3. Throughput of M radar network is given by,

$$\Theta = MLK\pi_1(1 - p_{I2})^{M-1} \quad (12)$$

Proof: From the definition of throughput (see 2.2), we have

$$\Theta = \lim_{T \rightarrow \infty} KL \frac{S(T)}{T},$$

where $S(T)$ total number of packets transmitted successfully by all radars in T time slots. Now consider a radar in the network. Let the total number of transmissions cycles until time slot T is given by $\phi(T)$. The average number of successful packets transmission cycles is given by $\phi(T)(1-p_{I2})^{M-1}$ and number of chirps transmitted is given by $L\phi(T)(1-p_{I2})^{M-1}$. In M independent radars network the average number of successful transmission cycles is given by $M\phi(T)(1-p_{I2})^{M-1}$. Using this we can write,

$$\begin{aligned} \Theta &= \lim_{T \rightarrow \infty} \frac{KML\phi(T)(1-p_{I2})^{M-1}}{T} \\ &= \frac{1}{KL + \mathbb{E}[W]} MKL(1-p_{I2})^{M-1} \\ &= MLK\pi_1(1-p_{I2})^{M-1} \end{aligned}$$

where the first and second equalities follow from Elementary Renewal and Renewal Reward theorems [16]. \square

3.4 p_I and p_{opt} for geometric backoff

In this section we present results obtained for geometric backoff distribution, $W \sim \text{Geo}(p)$ where p is the attempt probability and supported on the set $\{0, 1, 2, \dots\}$.

- 1) The probability of interference at the tagged radar in two radar network is given by,

$$\begin{aligned} p_{I2} &= (2L-1)\mathbb{P}(E_i) \\ &\quad - \frac{p^2}{pKL + 1 - p} \sum_{i=1}^{L-1} (L-i) \left(2(1-p)^{(i-1)K} \right. \\ &\quad \left. + (1-p)^{(i-1)K+1} + (1-p)^{(i-1)K-1} \right), \end{aligned}$$

where

$$\mathbb{P}(E_i) = \begin{cases} \frac{2}{KL + \mathbb{E}[W]} & \text{for } KL > 1 \\ \frac{1}{1 + \mathbb{E}[W]} + \frac{p\mathbb{E}[W]}{1 + \mathbb{E}[W]} & \text{for } KL = 1. \end{cases}$$

and $\mathbb{E}[W] = \frac{1-p}{p}$.

- 2) Further, we consider number of chirps per packet equal to one i.e., $L = 1$ and evaluate the attempt probability p_{opt} at which the network has the maximum throughput.

$$p_{opt} = \begin{cases} \frac{1}{2M+1-K}, & \text{if } 2M+1-K > 0 \\ 1, & \text{otherwise.} \end{cases}$$

We observe that a centralized transmission scheduling can achieve a throughput close to $\min\{K, M\}$ which is much more than the throughput achieved by ALOHA, e.g., see Figure 12b. This motivates us to explore other MAC protocols.

4 CSMA

In slotted ALOHA, the radars initiate transmissions irrespective of the activities of other radars. Consequently, in most of the scenarios, slotted ALOHA achieves a throughput far below the best possible values (see Figure 12b). This

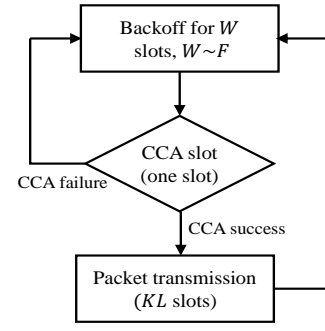


Fig. 8. CSMA, After every backoff radar senses the medium for f_{\min} (CCA), if CCA is successful then it transmits else enter into backoff

motivates us exploring other MAC protocols that account for other radars' activities. In this section, we study a MAC protocol in which a radar senses the medium following each backoff, and initiates a transmission only if the medium is sensed idle.

CSMA: In CSMA, a radar after each backoff, senses the medium for one slot which is referred to as clear channel assessment (CCA) slot. In the CCA slot, the radar sets the Tx chirp frequency input to the mixer to f_{\min} and observes the output of its LPF at the end of the CCA slot. If the radar observes a signal (of frequency less than f_H), it assumes the CCA to have failed and enters into another random backoff. If the radar does not observe a signal at the end of the CCA slot, it assumes the CCA to have succeeded and starts a packet transmission on completion of the CCA slot. We illustrate the flow chart of our CSMA protocol in Figure 8.

Remark 4.1. Note that if the radar observes a signal at the end of the CCA slot and still starts a packet transmission in the next slot, this packet would interfere with the packet that caused the observed signal. In other words a transmission following a CCA failure would certainly lead to interference. On the other hand, a transmission following a CCA success need not be interference free as we explain in Section 4.1.2.

Recall that in ALOHA each radar transmits packets irrespective of other radars' transmissions. But in CSMA all the radars' backoffs, CCAs and packet transmissions are coupled. In the following subsections we analyze CSMA in various cases.

4.1 Collocated radars

We consider a collocated and asynchronous radar network. Further, we first consider number of chirps per packet, L to be one. We consider $L > 1$ subsequently.

4.1.1 $L = 1$

In this case we observe that the radars do not suffer interference in CSMA. Observe that, in CSMA, for a CCA success at a radar, the immediately preceding chirp transmission by any of the other radars must have started at least Δ time before the end of the CCA slot. Consequently, start times of packet transmissions by the radars are separated by at least Δ , and so the packets will not interfere with each

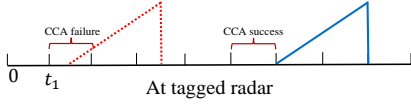


Fig. 9. Illustrating CCA success, CCA failure and packet transmission at the tagged radar in a collocated radar network for $L = 1, K = 2$

other. We illustrate it by showing sample CCA failure and CCA success events in Figure 9. Let t_1 be the CCA slot at the tagged radar. The tagged radar senses the f_{\min} of the chirp transmitted (dotted red color) by the interfering radar, experiences CCA failure as shown in Figure 9. The next CCA attempt is successful and tagged radar starts transmission immediately after the CCA slot.

In the following we compute the throughput. Let us consider a tagged radar. We assume that the backoffs are sampled from $\text{Geo}(p)$ distribution. Let $I_s(T)$ be the number of successful transmissions at the tagged radar until slot T . Further, let p_s be the conditional CCA success probability at the tagged radar i.e., the probability of CCA success given the tagged radar is in a CCA. We define the tagged radar's transmission rate and the aggregate throughput, p_r and Θ , respectively, as follows.

$$p_r := \lim_{T \rightarrow \infty} \frac{I_s(T)}{T}. \quad (13)$$

Using above and $L = 1$ in the definition of throughput 2.2 we have

$$\Theta = MKp_r. \quad (14)$$

Remark 4.2. Observe that the maximum throughput that can be achieved by any algorithm for $L = 1$ is $\min\{M, K\}$. Using this in (14) gives $p_r \leq \frac{1}{\max\{M, K\}}$.

In the following we compute the throughput using decoupling approximation and fixed point analysis [17], [18]. Towards this we find the relation between p_r, p_s in Lemma 4.1.

Lemma 4.1.

$$p_r = \frac{1}{K + \frac{1}{pp_s}}$$

Proof: Let us define the state of a radar in a slot as follows. We say that the radar is in state -1 if it is sensing the medium, state 0 if it is in backoff. Further, we say that radar is in state $i, 1 \leq i \leq K$ if it is transmitting i -th slot of the packet. The radar's state evolves according to a renewal process with the slots in which the radar state is 1 being the renewal epochs. Let the duration between any two renewal epochs i and $i + 1$ is given by D_i . Observe that $D_i, i \in \{1, 2, \dots\}$ is random and independent across i . Further, $\mathbb{E}[D_i] = K + \frac{1}{pp_s}$.

Using Elementary Renewal theorem [16],

$$\begin{aligned} p_r &= \lim_{T \rightarrow \infty} \frac{I_s(T)}{T} \\ &= \frac{1}{K + \frac{1}{pp_s}} \end{aligned}$$

almost surely. \square

To compute p_s we use the decoupling approximation [17], [18]. The decoupling approximation assumes that the aggregate attempt process of the other radars is independent of the backoff process of the tagged radar. Recall in any Δ interval of tagged radar's timeline, at most one radar can start packet transmission. The unconditional probability of any one among $M - 1$ radars starting transmission in one slot is given by $(M - 1)p_r$. The unconditional probability of no radar starting transmission is given by $1 - (M - 1)p_r$. From Remark 4.2 we observe that $1 - (M - 1)p_r > 0$. We want to calculate the conditional probability, p_s at the tagged radar i.e., given the tagged radar is in a CCA slot the probability of its CCA success. But we use the unconditional CCA success probability $1 - (M - 1)p_r$ for p_s in Lemma 4.1 to compute p_r . Further, we substitute p_r in (14) to compute the throughput.

$$p_r = \frac{1}{K + \frac{1}{p(1 - (M - 1)p_r)}}$$

For a given M, p we can write above as

$$p_r = f(p_r).$$

In Lemma 4.2 we show that p_r can be computed using fixed point analysis.

Lemma 4.2. For a $p_r = f(p_r)$ has a unique fixed point.

Proof:

- $f(\cdot)$ is a continuous map from $[0, \frac{1}{\max\{M, K\}}]$ to $[f(0), f(\frac{1}{\max\{M, K\}})]$ and decreasing in p_r
- $f(\frac{1}{\max\{M, K\}}) < \frac{1}{\max\{M, K\}}$

Hence by intermediate value theorem there exists a unique fixed point. \square

We use p_r obtained from Lemma 4.2 in (14) to compute the throughput. We find from Section 5 (see Figure 13b) that the throughput obtained from the fixed point analysis matches the simulation with less than 10 percent error for $M > K$. Further, from Figure 14 we observe that in CSMA the throughput increases in attempt probability, and for all values of p throughput of CSMA is better than ALOHA.

4.1.2 $L > 1$

We notice that when $L > 1$, packets may interfere under the proposed CSMA. We illustrate this using Figure 10. Let us assume that the tagged radar starts CCA at slot t_1 , while other radar transmitting a packet (dotted red color). The tagged radar CCA is successful as the starting time of other radar is earlier than t_1 . However the subsequent packet (solid blue color) transmission of the tagged radar is interfered by the the second chirp of the packet from the other radar. Observe that during interference one of the radar should be transmitting the first chirp in a packet and other must be transmitting chirp $j, 1 < j \leq L$ in a packet.

From simulation (see Figure 17) we observe that CSMA's throughput is higher than that of slotted ALOHA for all values of p . We also observe that the throughput is a non-monotonic function of p . \square

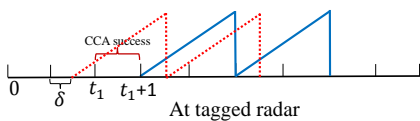


Fig. 10. Illustrating interference at the tagged radar after CCA success in a collocated radar network for $L = 2, K = 2$

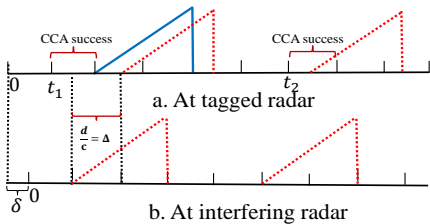


Fig. 11. Illustrating interference in a non-collocated radar network for $L = 1, K = 2$, a. Transmitted and received packets at the tagged radar, b. Transmitted packets at the interfering radar

4.2 Non-collocated radars

We consider a non-collocated and asynchronous radar network. In Section 4.1.1 we saw that in a collocated radar network radars do not suffer interference for $L = 1$. But in non-collocated setting radars suffer interference for $L = 1$ also. We explain this in the following using Figure 11. Let d be the distance between the tagged and interfering radars and $d < d_{I,\max}$. The tagged radar receives the packets transmitted by the interfering radar with a delay of $\frac{d}{c}$. Let $d = c\Delta$. This causes a delay of one slot as shown in Figure 11. Let us assume that the tagged radar started CCA at slot t_1 . In Figure 11 observe that though the interfering radar started a packet transmission during the CCA slot of the tagged radar, the tagged radar can not sense it because of the delay caused by the distance. The packet received at the tagged radar is shown in dotted lines (see Figure 11a). The packet transmitted by the interfering radar reached the tagged radar after the CCA slot. So, the CCA was successful and the tagged radar started the packet transmission at slot $t_1 + 1$. The tagged radar received the packet during the first slot of packet transmission and suffered interference.

Now consider another CCA slot at t_2 . The tagged radar senses the packet from the other radar, it is a CCA failure and packet transmission did not start at slot $t_2 + 1$. So, the CSMA avoids interference caused by packets that are received at the tagged radar in the CCA slot. From Section 5 (see Figure 20) we observe that for $L = 1$ in CSMA the throughput increases in p , and for all values of p throughput of CSMA is better than ALOHA.

5 NUMERICAL RESULTS

In this section, we simulate an FMCW radar network with M radars. The radars' clocks are not synchronized. Assume that there is a hypothetical global clock, the clock offsets for each radar is assumed to be uniformly distributed random variable in $[0, \Delta)$. More precisely, we consider the cases of collocated and non-collocated radars. In the case

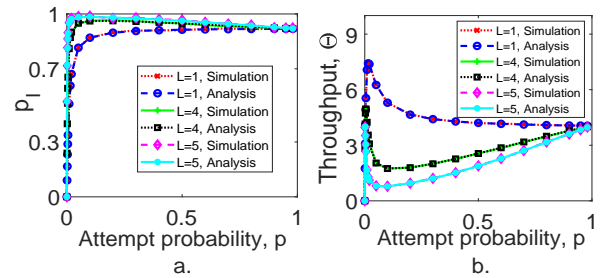


Fig. 12. Verifying the analytical results obtained in Propositions 2 and 3 for ALOHA, a. Probability of interference vs attempt probability, b. Throughput vs attempt probability for $M = 50, K = 40, L = 1, 4, 5$

of non-collocated radars, we assume that the radars are placed on a line segment $[0, d_{I,\max}]$. Radar locations are chosen from i.i.d. Uniform $[0, d_{I,\max}]$ distributions. We set $d_{I,\max} = 4d_{\max}$. We assume that backoffs are sampled from Geo(p) distribution.

We first verify the probability of interference (p_I) and throughput (Θ) obtained in Proposition 2 and Proposition 3, respectively for different values of packet length (L), attempt probability (p) and number of radars (M) in ALOHA. Then we verify the fixed point solution obtained in Lemma 4.2 for collocated radar networks by varying L, p, M in CSMA. Finally, we compare the performance of ALOHA and CSMA by varying L, p, M .

In Figure 12 we demonstrate how p_I and Θ vary with the attempt probability p and L in ALOHA. Towards this we consider a network with $M = 50$ radars with chirp length $K = 40$. Further, we consider $L = 1, 4, 5$.

We observe in Figure 12 that p_I, Θ obtained from simulation and analysis match very closely (less than 2 percent error). Further, we also observe that at $p = 1$, p_I and Θ do not vary with L . This is because, at $p = 1$, each radar generates a continuous train of packets with no backoff between them. We also observe that for $L > 1$ interference probability increases and then decreases with p which is different from wireless networks. Further, we find from Figure 12b that the maximum throughput for $L = 1$ is achieved at $p_{opt} = \frac{1}{2M+1-K} = 0.016$ (see Section 3.4).

In Figure 13 we demonstrate the fixed point solution obtained in Lemma 4.2 for CSMA and compare it with the simulation. Towards this we consider a radar network with $M = 50$ radars each using chirp length $K = 40$ and $L = 1$. In Figure 13a we plot fixed point solution for different attempt probabilities $p = 0.2, 0.4, 0.6$. In Figure 13b we plot throughput obtained from fixed point analysis and the simulation by varying p for $M = 30, 40, 50$. We find that the error in throughput obtained from the fixed point analysis matches the simulation with less than 10 percent error.

To compare the performance of ALOHA and CSMA we consider the following two network scenarios separately.

- collocated and asynchronous radar network,
- non-collocated and asynchronous radar network.

5.1 Collocated and asynchronous radar network

In this section, we simulate a collocated radar network. We first consider the case where the number of chirps per packet

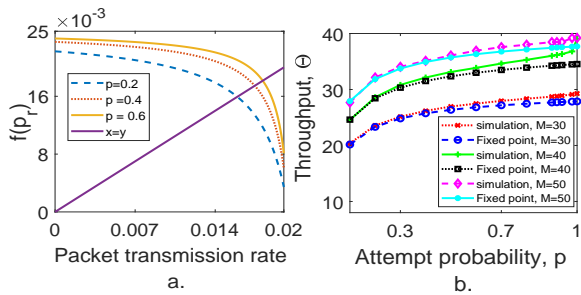


Fig. 13. a. Fixed point analysis for $M = 50, K = 40$, b. Throughput vs attempt probability for a collocated radar network $K = 40, L = 1$

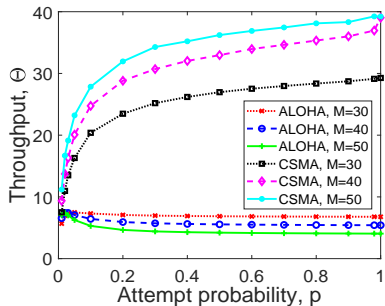


Fig. 14. Throughput vs attempt probability for collocated and asynchronous radar network, $L = 1, K = 40, M = 30, 40, 50$

$L = 1$. Subsequently, we consider $L > 1$ case.

5.1.1 $L = 1$

To begin with we demonstrate how the throughput varies with p . Towards this we fix $K = 40$ and vary M as shown in Figure 14. We observe that in CSMA the throughput increases in p . We observe that the network achieves maximum throughput at $p = 1$. We explain this in the following. Recall from Section 4.1.1 that in a collocated and asynchronous network radars suffer no interference. At $p = 1$ each radar continuously senses the medium until its CCA is successful i.e., the radar is either transmitting the packet or sensing the medium. Further, we observe that for $L = 1$ the maximum throughput that can be achieved is $\min\{M, K\}$. We find that in Figure 14 for $M = 30, 40, 50$ and $K = 40$ CSMA achieves 29.3, 39.1, 39.25 at $p = 1$ respectively. In ALOHA the throughput decreases with the increase in the number of radars after maximum throughput. This is because each radar transmits packets irrespective of other radar packet transmissions. So, at a higher value of attempt probability every radar transmits packets often and suffers interference. Further, we observe that CSMA has better throughput than ALOHA.

In Figure 15 we demonstrate how p_{opt} and Θ_{opt} vary with M for CSMA and ALOHA. Towards this, we fix $K = 40$. From Figure 14 we observed that in CSMA throughput increases in p , so observe $p_{opt} = 1$ for all values of M in Figure 15a. Further, in Figure 15b we observe that Θ_{opt} increases in M in CSMA though the increase is small. In ALOHA we observe that p_{opt} decreases with the increase in the number of radars. This is because for a fixed p , as the number of radars increase interference probability increases. So, radar has to transmit packets less often to

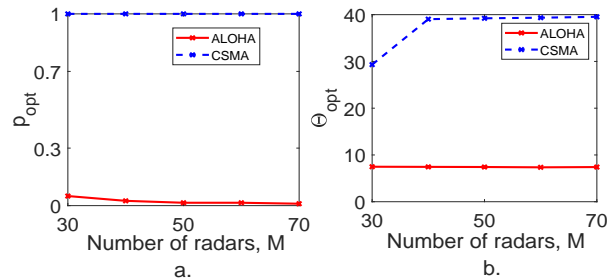


Fig. 15. a. p_{opt} vs number of radars, b. Θ_{opt} vs number of radars for collocated and asynchronous radar network, $L = 1, K = 40$

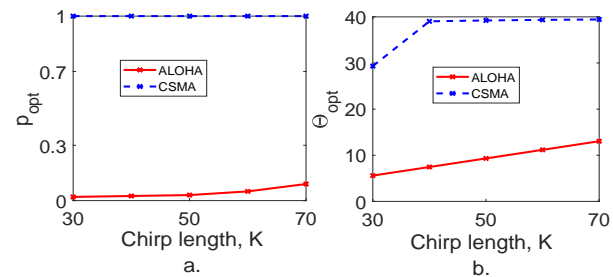


Fig. 16. a. p_{opt} vs chirp length, b. Θ_{opt} vs chirp length for collocated and asynchronous radar network, $L = 1, M = 40$

avoid interference, i.e., p has to decrease with the increase in M . From Figure 15b we find that θ_{opt} decreases with M in ALOHA though the decrease is small. Further, the optimum throughput achieved by CSMA is always more than the optimum throughput achieved by ALOHA.

In Figure 16 we demonstrate how p_{opt} and Θ_{opt} vary with K . Towards this we fix $M = 40$. From Figure 14 we observed $p_{opt} = 1$ for CSMA. From Figure 16b we observe that Θ_{opt} increases in K though the increase is small. From Figure 16b we observe that in ALOHA p_{opt} increases in K . This is because for a fixed p the probability of interference decreases with the increase in chirp length, K . So, we can increase p to achieve optimum throughput.

5.1.2 $L > 1$

To begin with, we demonstrate how the throughput varies with p . Towards this, we fix $K = 40, L = 4$ and vary M as shown in Figure 17. In both the protocols we observe that throughput is less compared with $L = 1$ (Figure 14). We explain this in the following. In CSMA for $L = 1$ the radars suffer no interference (see Section 4.1.1). For $L > 1$ radars suffer interference and this deteriorates the throughput. In ALOHA for a given p, M , interference probability increases in L . So, the throughput is less compared to the case $L = 1$.

In Figure 18 we demonstrate how p_{opt} and Θ_{opt} vary with M in the network for CSMA and ALOHA. In Figure 18a we observe that p_{opt} decreases with the increase in M in both CSMA and ALOHA. This is because, for a given p , the interference probability increases with the increase in M . So, the radar has to participate less aggressively in transmitting the packets. Further, in Figure 18b we observe a decrease in throughput with the increase in M for both CSMA and ALOHA. This is because for a fixed p interfer-

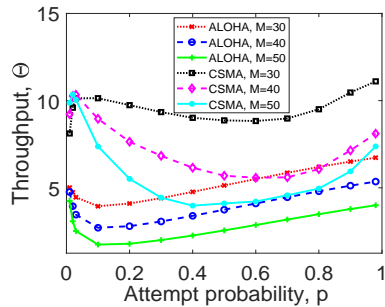


Fig. 17. Throughput vs attempt probability for collocated and asynchronous radar network, $L = 4, K = 40, M = 30, 40, 50$

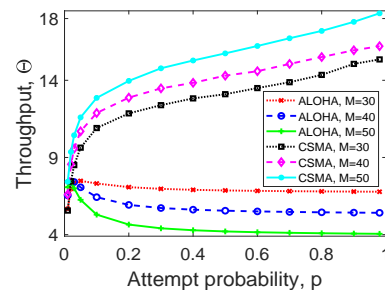


Fig. 20. Throughput vs attempt probability for non-collocated and asynchronous radar network, $L = 1, K = 40, M = 30, 40, 50$

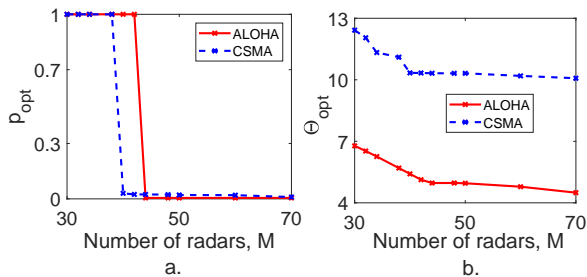


Fig. 18. a. p_{opt} vs number of radars, b. Θ_{opt} vs number of radars for collocated and asynchronous radar network, $L = 4, K = 40$

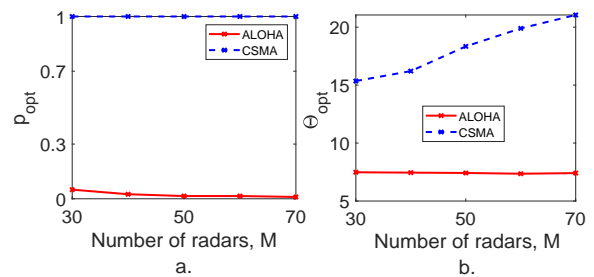


Fig. 21. a. p_{opt} vs number of radars, b. Θ_{opt} vs number of radars for non-collocated and asynchronous radar network, $L = 1, K = 40$

ence probability increases in M so the throughput decreases.

In Figure 19 we demonstrate how p_{opt} and Θ_{opt} vary with chirp length for CSMA and ALOHA. In Figure 19a we observe that p_{opt} increases in K for both CSMA and ALOHA. This is because for a given p , M interference probability decrease with chirp length, K . So, we can increase p to achieve optimum throughput. In Figure 19b we observe that Θ_{opt} increases in K for both CSMA and ALOHA.

5.2 Non-collocated and asynchronous radar network

In this section, we simulate a collocated radar network. We first consider the case where the number of chirps per packet $L = 1$. Subsequently, we consider $L > 1$ case.

5.2.1 $L = 1$

To begin with we demonstrate how the throughput varies with p . Towards this we fix $K = 40$ and vary M as shown in Figure 20. We observe that in CSMA the throughput

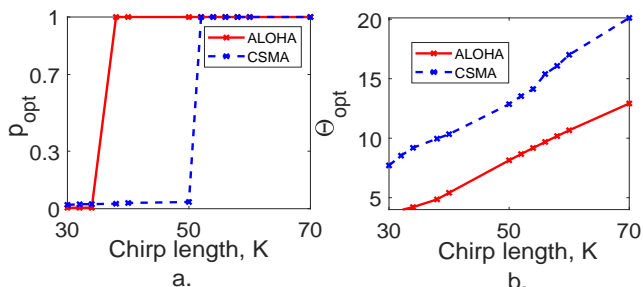


Fig. 19. a. p_{opt} vs chirp length, b. Θ_{opt} vs chirp length for collocated and asynchronous radar network, $L = 4, M = 40$,

increases in p . However, it is less compared to the case $L = 1$ collocated radar network at all the values of p (see Figure 14). This is because in CSMA, the radars do not suffer interference when they are collocated but they suffer interference when they are not collocated. In ALOHA the throughputs are the same in collocated and non-collocated radar networks. This is because the radars do not sense the medium in ALOHA and each radar transmits packets irrespective of other radars' transmissions.

In Figure 21 we demonstrate how p_{opt} and Θ_{opt} vary with M in CSMA and ALOHA. In Figure 20 we observed that in CSMA throughput increases in p . So, in Figure 21a we observe $p_{opt} = 1$ for CSMA. In Figure 21b we observe that throughput increases in M , in CSMA. In ALOHA, given network parameters L, K, M, p throughputs are the same for collocated and non-collocated networks. So, the same observations made for collocated network in ALOHA apply here (see Section 5.1.1).

In Figure 22 we demonstrate how p_{opt} and Θ_{opt} vary with chirp length in CSMA and ALOHA. In Figure 22a we observe that $p_{opt} = 1$ for CSMA. In Figure 22b we observe that throughput increases in K in CSMA. This is because the probability of interference decreases with the increase in K . So, the throughput increases.

5.2.2 $L > 1$

To begin with, we demonstrate how the throughput varies with p . Towards this, we fix $K = 40, L = 4$ and vary M as shown in Figure 23. In Figure 23 we observe that the throughput in CSMA is less compared to the case of collocated radar network $L = 4$ at all the values of p (see Figure 17). This is because the probability of interference increases in L . So, the throughput decreases. In ALOHA,

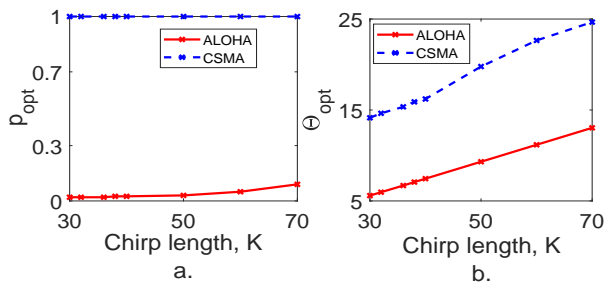


Fig. 22. a. p_{opt} vs chirp length, b. Θ_{opt} vs chirp length for non-collocated and asynchronous radar network, $L = 1$, $M = 40$,

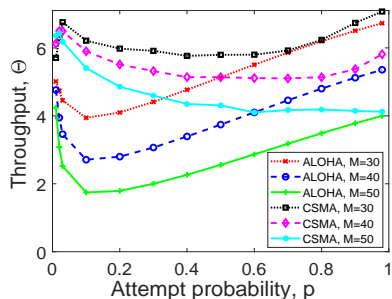


Fig. 23. Throughput of slotted CSMA and slotted ALOHA for non-collocated radar network with asynchronous clock, $L = 4$, $K = 40$, $M = 30, 40, 50$

given network parameters, L, K, M, p throughputs are the same for collocated and non-collocated networks. So, the same observations made for collocated networks in ALOHA are hold here (see Section 4.1.2).

In Figure 24 we demonstrate how p_{opt} and Θ_{opt} vary with M in CSMA and ALOHA. In Figure 24a we observe that p_{opt} decreases with M in both CSMA and ALOHA. This is because as the number of radars increases in the network the interference probability also increases. So, the radar has to participate less aggressively in transmitting the packets. Further, in Figure 18b we observe a decrease in throughput with the increase in the number of radars, M for both CSMA and ALOHA. This is because for a given p the interference probability increases in M . So, the throughput decreases.

In Figure 25 we demonstrate how p_{opt} and Θ_{opt} vary with chirp length for CSMA and ALOHA. In Figure 25a we observe that p_{opt} increases in K for both CSMA and ALOHA. This is because, for a given p, M interference

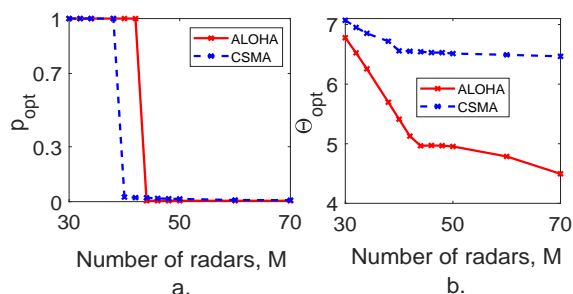


Fig. 24. a. p_{opt} vs number of radars, b. Θ_{opt} vs number of radars for non-collocated and asynchronous radar network, $L = 4$, $K = 40$

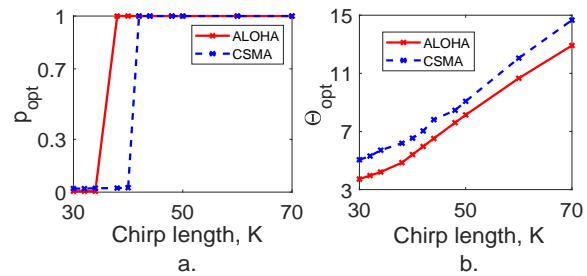


Fig. 25. a. p_{opt} vs chirp length, b. Θ_{opt} vs chirp length for non-collocated and asynchronous radar network, $L = 4$, $M = 40$

probability decreases with the increase in K . So, radars can aggressively participate in the packet transmission and we can improve the throughput. So, in Figure 25b we observe the increase in Θ_{opt} with chirp length for both CSMA and ALOHA.

6 CONCLUSION

We studied medium access in FMCW radar networks in which all the radars used the same parameters, e.g., chirp duration, chirp slope, cutoff frequency, number of chirps per packet, etc. We proposed and analyzed slotted ALOHA and CSMA protocols in terms of interference probability and throughput. In either case, we observed that interference probability and throughput may behave differently than in wireless communication networks. For instance, in the case of ALOHA, if the number of chirps per packet is larger than one, the interference probabilities may be smaller for higher transmission rates (see Figure 12a) and throughputs may be maximum at the highest possible transmission rates (see Figure 12b). In the case of CSMA also, using the highest possible attempt rates may maximize throughput (see Figure 14). We observed that CSMA outperformed ALOHA in all the realistic scenarios.

If the radars in a FMCW network use different chirp slopes, they may also be subject to wideband interference from other radars. Designing medium access protocols that also consider wideband interference is a challenging open problem. Usually, the received signals at the radars undergo further processing for estimation of object locations, velocities, etc (see [6]). The notions of interference probability and throughput can be refined to account for the detection and estimation errors. Designing medium access protocols that optimize the refined notion of throughput is another potential future direction.

REFERENCES

- [1] TI, Introduction to mmwave sensing:FMCW radars. URL <https://training.ti.com/intro-mmwave-sensing-fmcw-radars-module-1-r>
- [2] TI, mmwave radar for automotive and industrial applications. URL <https://training.ti.com/epd-pro-rap-mmwaveradar-adh-tr-webinar-eu>
- [3] C. Aydogdu, M. F. Keskin, G. K. Carvajal, O. Eriksson, H. Hellsten, H. Herbertsson, E. Nilsson, M. Rydstrom, K. Vanas, H. Wymeersch, Radar interference mitigation for automated driving: Exploring proactive strategies, IEEE Signal Processing Magazine 37 (4) (2020) 72–84. doi:10.1109/MSP.2020.2969319.
- [4] S. Rao, A. V. Mani, Interference characterization in FMCW radars, in: 2020 IEEE Radar Conference (RadarConf20), 2020, pp. 1–6. doi:10.1109/RadarConf2043947.2020.9266283.

- [5] S. Sun, A. P. Petropulu, H. V. Poor, MIMO radar for advanced driver-assistance systems and autonomous driving: Advantages and challenges, *IEEE Signal Processing Magazine* 37 (4) (2020) 98–117. doi:10.1109/MSP.2020.2978507.
- [6] S. Jin, S. Roy, Cross-layer interference modeling and performance analysis in FMCW radar multiple access network, in: 2020 IEEE 92nd Vehicular Technology Conference (VTC2020-Fall), 2020, pp. 1–6. doi:10.1109/VTC2020-Fall149728.2020.9348730.
- [7] S. Ishikawa, M. Kurosawa, M. Umehira, X. Wang, S. Takeda, H. Kuroda, Packet-based FMCW radar using CSMA technique to avoid narrowband interference, in: 2019 International Radar Conference (RADAR), 2019, pp. 1–5. doi:10.1109/RADAR41533.2019.171379.
- [8] D. Ammen, M. Umehira, X. Wang, S. Takeda, H. Kuroda, A ghost target suppression technique using interference replica for automotive FMCW radars, in: 2020 IEEE Radar Conference, 2020, pp. 1–5. doi:10.1109/RadarConf2043947.2020.9266514.
- [9] C. Aydogdu, M. F. Keskin, N. Garcia, H. Wymeersch, D. W. Bliss, RadChat: Spectrum sharing for automotive radar interference mitigation, *IEEE Transactions on Intelligent Transportation Systems* 22 (1) (2021) 416–429. doi:10.1109/TITS.2019.2959881.
- [10] S. Jin, S. Roy, FMCW radar network: Multiple access and interference mitigation, *IEEE Journal of Selected Topics in Signal Processing* 15 (4) (2021) 968–979. doi:10.1109/JSTSP.2021.3071565.
- [11] T. N. Luo, C.-H. E. Wu, Y.-J. E. Chen, A 77-GHz CMOS automotive radar transceiver with anti-interference function, *IEEE Transactions on Circuits and Systems I: Regular Papers* 60 (12) (2013) 3247–3255. doi:10.1109/TCSI.2013.2265974.
- [12] J. Khoury, R. Ramanathan, D. McCloskey, R. Smith, T. Campbell, RadarMAC: Mitigating radar interference in self-driving cars, in: 2016 13th Annual IEEE International Conference on Sensing, Communication, and Networking (SECON), 2016, pp. 1–9. doi:10.1109/SAHCN.2016.7733011.
- [13] K. U. Mazher, R. W. Heath, K. Gulati, J. Li, Automotive radar interference characterization and reduction by partial coordination, in: 2020 IEEE Radar Conference (RadarConf20), 2020, pp. 1–6. doi:10.1109/RadarConf2043947.2020.9266425.
- [14] Y. S. Son, H. K. Sung, S. W. Heo, Automotive frequency modulated continuous wave radar interference reduction using per-vehicle chirp sequences, *Sensors* 15 (3) (2018) 1–11. doi:10.3390/s18092831.
- [15] A. Al-Hourani, R. J. Evans, S. Kandeepan, B. Moran, H. Eltom, Stochastic geometry methods for modeling automotive radar interference, *IEEE Transactions on Intelligent Transportation Systems* 19 (2) (2018) 333–344. doi:10.1109/TITS.2016.2632309.
- [16] A. Kumar, Discrete event stochastic processes, lecture notes for engineering curriculum (2012). URL <https://ece.iisc.ac.in/anurag/index.php/books/>
- [17] A. Kumar, E. Altman, D. Miorandi, M. Goyal, New insights from a fixed-point analysis of single cell IEEE 802.11 WLANs, *IEEE/ACM Transactions on Networking* 15 (3) (2007) 588–601. doi:10.1109/TNET.2007.893091.
- [18] G. Bianchi, Performance analysis of the IEEE 802.11 distributed coordination function, *IEEE Journal on Selected Areas in Communications* 18 (3) (2000) 535–547. doi:10.1109/49.840210.